

BAYESIAN NARROWBAND INTERFERENCE MITIGATION IN SC-FDMA

Anum Ali¹, Mudassir Masood¹, Samir Al-Ghadhban² and Tareq Y. Al-Naffouri^{1,2}

¹Department of Electrical Engineering,
King Abdullah University of Science and Technology (KAUST), Saudi Arabia.

²Department of Electrical Engineering,
King Fahd University of Petroleum and Minerals (KFUPM), Saudi Arabia.
{anum.ali,mudassir.masood,tareq.alnaffouri}@kaust.edu.sa, samir@kfupm.edu.sa

ABSTRACT

This paper presents a novel narrowband interference (NBI) mitigation scheme for SC-FDMA systems. The proposed scheme exploits the frequency domain sparsity of the unknown NBI signal and adopts a low complexity Bayesian sparse recovery procedure. In practice, however, the sparsity of the NBI is destroyed by a grid mismatch between NBI sources and SC-FDMA system. Towards this end, an accurate grid mismatch model is presented and a sparsifying transform is utilized to restore the sparsity of the unknown signal. Numerical results are presented that depict the suitability of the proposed scheme for NBI mitigation.

Index Terms— NBI mitigation, Bayesian sparse recovery, SC-FDMA, compressed sensing, LTE.

1. INTRODUCTION

Single carrier - frequency division multiple access (SC-FDMA) has been adopted as the uplink multiple access scheme in 3GPP long term evolution, due to its robustness against multipath fading and low peak-to-average power ratio [1]. However, the wideband nature of SC-FDMA makes it highly susceptible to narrowband interference (NBI). The NBI sources include other devices operating in the same spectrum (e.g., cordless phones, garage openers etc.) and communication systems operating in a cognitive manner. At high signal-to-interference ratio (SIR), coding can be used to mitigate the errors introduced by the NBI. However, at low SIR levels, interference begins to overwhelm the code and necessitates a receiver that is able to directly deal with it.

In this work, we exploit the sparse nature of the NBI to recover it using a low complexity Bayesian sparse reconstruction procedure. Specifically, we utilize the recently proposed support agnostic Bayesian matching pursuit (SABMP) [2] algorithm for NBI recovery. The SABMP algorithm uses the statistics of additive noise (which is assumed Gaussian), but is agnostic to the distribution of the NBI - which is usually not known at the victim receiver. Further, the practical scenario of grid mismatch is also considered and the spreading effect is more realistically modelled by allowing the various NBI sources to have independent grid offsets. It is noted that the spectral spillover caused by the grid mismatch destroys the sparsity of the unknown signal. Hence, in this work, we utilize the *Haar* transform as a sparsifying transform to sparsify the unknown NBI signal.

The problem of NBI mitigation in OFDMA is the dual of impulsive noise cancellation problem [3] and is relatively well studied (see e.g., [4–6]). However, techniques developed for OFDMA do not readily apply to SC-FDMA as the

two systems are fundamentally different. The literature addressing the problem of NBI specifically for SC-FDMA is seriously limited and only a handful of articles are available (e.g., [7, 8]). Furthermore, these articles address specific cases (e.g., single NBI sources that don't change much over multiple symbols) under idealistic assumptions (e.g., known power and location). In this relation, the proposed scheme is distinguishable from existing literature as it aims at a general scenario of time-varying (changing completely from symbol-to-symbol) multiple NBI sources with independent grid offsets where no knowledge of the NBI location or power is assumed. Though [6] and [9] exploit the sparsity of unknown NBI for its mitigation, their work targets single-user zero padded - OFDM systems, whereas the proposed scheme is tailor made for multi-user SC-FDMA systems. Further, the proposed scheme is low complexity (unlike [9] that opted for ℓ_1 -optimization), and doesn't require the statistics of the unknown (unlike [6] that assumes Gaussian prior on the unknown and availability of second order statistics).

The remainder of the paper is organized as follows: Section 2 introduces the data model for NBI impaired SC-FDMA transmission. To mitigate the NBI, a Bayesian sparse recovery procedure is presented in Section 3. Simulation results are presented in Section 4 and Section 5 concludes the paper.

We set the stage by introducing our notation. Scalars, time domain vectors, frequency domain vectors, and matrices are represented respectively by italic letters (e.g., N), Bold-face lower-case letters (e.g., \mathbf{x}), bold-face upper-case calligraphic letters (e.g., \mathcal{X}), and Bold-face upper-case letters (e.g., \mathbf{X}). The symbols $\hat{\mathbf{x}}$, \mathbf{x}^H , $x(i)$, and $x^*(i)$ represent the estimate, hermitian (conjugate transpose), i th entry, and the conjugated i th entry of the vector \mathbf{x} . The cardinality of a set \mathcal{T} will be denoted by $|\mathcal{T}|$. Further, $\mathbb{E}[\cdot]$, \mathbf{I} , and $\mathbf{0}$ denote the expectation operator, identity matrix, and the zero vector, respectively.

2. SC-FDMA AND NBI MODEL

Consider an uplink SC-FDMA system with U users. In such a system, the u th user converts the incoming high rate bit stream into P parallel streams. These low rate bit streams are modulated using a Q -ary QAM alphabet $\{\mathcal{A}_0, \mathcal{A}_1, \dots, \mathcal{A}_{Q-1}\}$, resulting in a P dimensional data vector \mathbf{x}_u . The data \mathbf{x}_u is Fourier pre-coded using the $P \times P$ discrete Fourier matrix \mathbf{F}_P to lower the PAPR of the transmission signal. The (k, l) th element of \mathbf{F}_P is given by

$$f_P(k, l) = P^{-1/2} \exp\left(-j \frac{2\pi kl}{P}\right), \quad k, l \in 0, 1, \dots, P-1. \quad (1)$$

The pre-coded data $\mathbf{F}_P \mathbf{x}_u$ is now mapped to the sub-carriers designated for the u th user. In this work, we use interleaved

resource allocation due to the robustness of this setting to frequency selective fading [1]. For the u th user, the data $\mathbf{F}_P \mathbf{x}_u$ is mapped to the designated sub-carriers by using an $N \times P$ ($N = PU$) resource allocation matrix \mathbf{M}_u . For interleaved assignment, the (k, l) th element of \mathbf{M}_u is given by

$$m_u(k, l) = \begin{cases} 1, & k = u + Ul, \quad 0 \leq l \leq P - 1, \\ 0, & \text{otherwise.} \end{cases} \quad (2)$$

This makes the resource allocation matrices belonging to different users orthonormal, i.e., $\mathbf{M}_i^H \mathbf{M}_j = \mathbf{I}_P$, when $i = j$ and $\mathbf{0}_P$, when $i \neq j$. Now, the N dimensional inverse DFT (IDFT) operation (i.e., \mathbf{F}_N^H) on $\mathcal{X}_u = \mathbf{M}_u \mathbf{F}_P \mathbf{x}_u$ results in the desired time domain transmission signal. After adding the cyclic prefix, the time domain signal is fed to a finite impulse response channel of length N_c , $\mathbf{h}_u = [h_u^*(0), h_u^*(1), \dots, h_u^*(N_c - 1)]^H$. The channel tap coefficients form a zero mean, complex Gaussian, i.i.d collection. After removing the cyclic prefixes at the base-station (BS), the received time domain signal (in the absence of NBI) can be written as¹

$$\mathbf{y} = \sum_{u=0}^{U-1} \mathbf{H}_u \mathbf{F}_N^H \mathcal{X}_u + \mathbf{z}, \quad (3)$$

where \mathbf{H}_u is the circulant channel matrix for the u th user and \mathbf{z} is the additive white Gaussian noise (AWGN) with $\mathbf{z} \sim \mathcal{CN}(\mathbf{0}, \sigma_z^2 \mathbf{I}_N)$. The circulant nature of \mathbf{H}_u allows us to diagonalize it using the DFT matrix \mathbf{F}_N and write $\mathbf{H}_u = \mathbf{F}_N^H \mathbf{\Lambda}_u \mathbf{F}_N$, where $\mathbf{\Lambda}_u$ is a diagonal matrix with channel frequency response on its diagonal. In this work, the channel impulse response is assumed known at the receiver and hence \mathbf{H}_u and $\mathbf{\Lambda}_u$ are readily available. The frequency domain received data vector \mathcal{Y} is now given by

$$\mathcal{Y} = \mathbf{F}_N \mathbf{y} = \sum_{u=0}^{U-1} \mathbf{\Lambda}_u \mathcal{X}_u + \mathcal{Z}, \quad (4)$$

where $\mathbf{\Lambda}_u = \mathbf{F}_N \mathbf{H}_u \mathbf{F}_N^H$ and $\mathcal{Z} = \mathbf{F}_N \mathbf{z}$. At the receiver, the data vector \mathbf{x}_u can be estimated using the minimum mean square error - frequency domain equalization (MMSE-FDE) [11] to obtain the following estimate

$$\hat{\mathbf{x}}_u = \mathbf{R}_x \mathbf{A}^H (\mathbf{A} \mathbf{R}_x \mathbf{A}^H + \sigma_z^2 \mathbf{I})^{-1} \mathbf{M}_u^H \mathcal{Y}, \quad (5)$$

where $\mathbf{R}_x \triangleq \mathbb{E}[\mathbf{x}_u \mathbf{x}_u^H] = \sigma_x^2 \mathbf{I}$ is the auto-correlation matrix of the data vector and $\mathbf{A} \triangleq \mathbf{M}_u^H \mathbf{\Lambda}_u \mathbf{M}_u \mathbf{F}_P$. As MMSE estimator is linear in \mathcal{Y} , we can simply write $\hat{\mathbf{x}}_u = \mathbf{E}_u \mathcal{Y}$, where $\mathbf{E}_u = \sigma_x^2 \mathbf{A}^H (\sigma_x^2 \mathbf{A} \mathbf{A}^H + \sigma_z^2 \mathbf{I})^{-1} \mathbf{M}_u^H$. Using the definition of \mathbf{E}_u , we can write an approximate equality $\hat{\mathbf{x}}_u = \mathbf{x}_u + \mathbf{E}_u \mathcal{Z}$, which is true because $\mathbf{E}_u \mathbf{\Lambda}_u \mathbf{M}_u \mathbf{F}_P \approx \mathbf{I}$ (the approximation tends to equality as $\sigma_z^2 \rightarrow 0$).

In the following subsection, we explain how the NBI affects the SC-FDMA system.

2.1. The NBI Impaired SC-FDMA

The received SC-FDMA signal might be impaired by a single or multiple time-variant NBI sources. Let \mathcal{I}_L be an L dimensional vector representing the active NBI sources. Using \mathcal{I}_L , we obtain an N dimensional NBI signal $\mathcal{I} = \mathbf{F}_N \bar{\mathbf{F}}_N^H \mathcal{I}_L$, where $\bar{\mathbf{F}}_N^H$ is an $N \times L$ partial IDFT matrix containing the columns corresponding to the frequencies of active NBI sources. Here, it is important to understand that channels between the NBI sources and the BS are absorbed into \mathcal{I}_L .

In other words, we can say that $\mathcal{I}_L = \mathbf{\Lambda}_{\mathcal{I}_L} \bar{\mathcal{I}}_L$, where $\mathbf{\Lambda}_{\mathcal{I}_L}$ is a diagonal $L \times L$ matrix containing the frequency domain channel gains between the interference sources and the receiver antennas, where $\bar{\mathcal{I}}_L$ represents the actual interference sources. Hence, a simple addition of \mathcal{I} in (4) will yield the NBI impaired SC-FDMA received signal. This received signal is given as

$$\mathcal{Y} = \sum_{u=0}^{U-1} \mathbf{\Lambda}_u \mathcal{X}_u + \mathcal{I} + \mathcal{Z}. \quad (6)$$

In practice, the NBI sources may have a grid offset with the SC-FDMA system, causing the energy of the NBI to spill over all tones. A spreading matrix $\mathbf{H}_{fo} = \mathbf{F}_N \mathbf{\Lambda}_{fo} \mathbf{F}_N^H$ is commonly used to model the grid offset between the NBI signal and the system under consideration [6, 9]. The diagonal matrix $\mathbf{\Lambda}_{fo}$ is defined as $\mathbf{\Lambda}_{fo} \triangleq \text{diag}(1, \exp(j \frac{2\pi\alpha(1)}{N}), \dots, \exp(j \frac{2\pi\alpha(N-1)}{N}))$, where α is a random number uniformly distributed over the interval $[-\frac{1}{2}, \frac{1}{2}]$. A fundamental limitation of this model is its inability to assume independent grid offsets for multiple NBI sources. To overcome this limitation, we define the spread NBI signal as

$$\mathcal{I} = \mathbf{F}_N \bar{\mathbf{F}}_{con}^H \mathcal{I}_L, \quad (7)$$

where $\bar{\mathbf{F}}_{con}$ is the $L \times N$ continuous DFT matrix, with (f_l, k) th entry

$$\bar{\mathbf{F}}_{con, (f_l, k)} = N^{-1/2} \exp\left(-j \frac{2\pi f_l k}{N}\right), \quad l \in 0, 1, \dots, L-1, \quad k \in 0, 1, \dots, N-1. \quad (8)$$

As the normalized frequencies $f_l/N \in [0, 1)$ are drawn independently, they emulate independent grid offsets for different NBI sources. Recently, Tang *et al.* used a similar modelling approach in an attempt to estimate continuous frequencies and amplitudes of a mixture of complex sinusoids [12].

The estimate of the transmitted signal \mathbf{x}_u in NBI free case (i.e., (4)) is obtained using (5). However, following the same estimation procedure for NBI impaired system (i.e., (6)) will yield

$$\hat{\mathbf{x}}_u = \mathbf{x}_u + \mathbf{E}_u (\mathcal{I} + \mathcal{Z}), \quad (9)$$

which is not a reliable estimate of \mathbf{x}_u due to the presence of \mathcal{I} . Further, note that \mathcal{I} perturbs \mathbf{x}_u through an IDFT operation (as evident by giving a closer look to the construction of \mathbf{E}_u), hence, even in the optimistic case (i.e., a single NBI source with no grid offset) all data points are corrupted by the NBI. In low SIR scenarios, the interference might be strong enough to take a majority of data symbols out of their correct decision regions, resulting in an intolerably high BER. Thus, our task is the estimation/mitigation of \mathcal{I} , which we pursue using a Bayesian sparse recovery framework.

3. BAYESIAN SPARSE RECOVERY OF THE NBI

To reconstruct the unknown NBI signal, we keep a randomly chosen subset of the vector \mathbf{x}_u data free and index this subset using \mathcal{T}_u . To extract the portion of the received signal corresponding to the reserved tones, let us define a $|\mathcal{T}_u| \times P$ binary selection matrix $\mathbf{S}_{\mathcal{T}_u}$. The selection matrix $\mathbf{S}_{\mathcal{T}_u}$ has one entry equal to 1 per row, corresponding to the location of a reserved data point (with all other entries being zero). Now we proceed by projecting $\hat{\mathbf{x}}_u$ (defined in (9)) onto the subspace spanned by the reserved points, i.e.,

$$\underbrace{\mathbf{S}_{\mathcal{T}_u} \hat{\mathbf{x}}_u}_{\mathbf{x}'_{u, \mathcal{T}}} = \mathbf{S}_{\mathcal{T}_u} \mathbf{x}_u + \underbrace{\mathbf{S}_{\mathcal{T}_u} \mathbf{E}_u}_{\mathbf{\Psi}_{u, \mathcal{T}}} (\underbrace{\mathcal{I} + \mathcal{Z}}_{\mathcal{I}'}), \Rightarrow \mathbf{x}'_{u, \mathcal{T}} = \mathbf{\Psi}_{u, \mathcal{T}} \mathcal{I}', \quad (10)$$

¹Bayesian NBI mitigation for SIMO systems is addressed in [10].

where $\mathbf{S}_{\mathcal{T}_u} \mathbf{x}_u = \mathbf{0}$. At this stage, we drop the subscript u for notational convenience and simply write $\mathbf{x}'_{\mathcal{T}} = \Psi_{\mathcal{T}} \mathcal{I}'$. To recover \mathcal{I} , the above under-determined system of equations can be solved using any compressed sensing (CS) reconstruction algorithm (e.g., [13–17]). In this work, we follow a Bayesian sparse recovery framework for the estimation of the unknown NBI signal. However, Bayesian sparse NBI recovery poses a couple of fundamental challenges: i) Common Bayesian approaches assume a known prior on the active elements of the unknown signal (see e.g., [14, 18]), whereas, we may not know the distribution of the NBI and ii) The sparsity of the NBI signal is destroyed due to the grid offset, These problems are addressed below.

Prior on \mathcal{I}' : Common Bayesian schemes assume a known prior on the unknown signal, e.g., [18] assumes a Laplacian prior. However, in practice i) we may not know the distribution of \mathcal{I} and ii) even if we did know the distribution, it might be difficult to estimate its parameters (i.e., moments). Towards this end, let us recall that \mathcal{I}_L represents the joint channel-NBI source i.e., $\mathcal{I}_L = \Lambda_{\mathcal{I}_L} \tilde{\mathcal{I}}_L$. Hence, if we assume circularly symmetric complex Gaussian prior for both $\tilde{\mathcal{I}}_L$ and Λ_{NBI} , then the entries of \mathcal{I}_L are formed by the product of two independent complex normal random variables i.e., *complex Double Gaussian* [19]. Hence, in this case, though the distribution is known, its parameter estimation is relatively difficult. Further, if non-Gaussianity is assumed on the NBI-BS channel model, it may yield more complex statistical behaviour for \mathcal{I}_L . As we are interested in recovering \mathcal{I} , we note that for no grid offset, the active elements of \mathcal{I} will assume the distribution of \mathcal{I}_L . However, grid offset will make the statistical characterization of \mathcal{I} even more challenging. For these reasons, a suitable reconstruction scheme would be able to work regardless of the distribution of unknown signal and whether this distribution is known or not. To this end, note that SABMP algorithm [2] is agnostic to the distribution of active taps - but acknowledges the sparsity of the unknown vector and Gaussianity of the additive noise. Further, SABMP has been shown to outperform many algorithms [2], and is successfully applied in several applications (e.g., [20, 21]). Hence, in this work we employ SABMP as a sparse NBI recovery scheme.

Sparsifying \mathcal{I}' : A fundamental requirement of sub-Nyquist sampling based reconstruction (as pursued in this work) is the sparsity of the unknown signal. Though there are only a few active NBI sources, in practice, the non-orthogonality of these sources to the SC-FDMA grid destroys the frequency domain sparsity of the unknown signal. Two strategies are followed in literature to tackle the grid offset problem. One possibility is to estimate the grid offset (see e.g., [22, 23]), however, estimation is complicated as offset is a highly nonlinear function of the observations \mathcal{Y} and different NBI sources assume independent grid offsets. The second approach is more mainstream and directly deals with an NBI signal experiencing energy spill-over (due to the grid mismatch) by *windowing* [9]. A windowing matrix function $\mathbf{H}_{win} = \mathbf{F}_N \Lambda_w \mathbf{F}_N^H$ applied to the received signal sparsifies the unknown vector \mathcal{I}' . Here, $\Lambda_w \triangleq \text{diag}(w(0), w(1), \dots, w(N-1))$ and $w(n)$ is the n th sample of the window function. It is a common practice to window the received time domain signal before taking the DFT. However, since the sole purpose of introducing windowing is enhancing the sparsity of \mathcal{I}' , we can postpone its inclusion till NBI reconstruction. To incorporate the window-

ing matrix function at NBI recovery stage we can re-write (10) as

$$\mathbf{x}'_{\mathcal{T}} = \Psi_{\mathcal{T}} \mathbf{H}_{win}^{-1} \mathbf{H}_{win} \mathcal{I}', \quad (11)$$

where we assume the non-singularity of \mathbf{H}_{win} . Now, if we sense via $\Psi_{\mathcal{T}} \mathbf{H}_{win}^{-1}$, we will be reconstructing $\mathbf{H}_{win} \mathcal{I}'$, which is more sparse compared to \mathcal{I}' . As the formulation (11) requires only the non-singularity of \mathbf{H}_{win} , we are motivated to look for other possibilities towards sparsifying \mathcal{I}' . Our drive to seek a better replacement for \mathbf{H}_{win} also stems from the fact that \mathbf{H}_{win} is not a unitary matrix and hence lacks a very desirable property pertaining to dictionary design in standard CS [24]. In this relation, any transformation matrix that is; i) linear, ii) non-singular, iii) unitary and iv) a good choice for sparsifying NBI, will serve the purpose. While choosing a sparsifying transform for NBI reconstruction, though properties i), ii) and iii) will be promptly evident, property iv) needs some consideration. To this end, note that unlike sparse signals, *compressible signals* (such as the NBI under grid offset) cannot be compared using ℓ_0 norm. As $\|\mathcal{I}'\|_{\ell_0} = \|\mathbf{H}_{win} \mathcal{I}'\|_{\ell_0} = N$, counting the number of active elements will yield a false conclusion that windowing did not enhance the sparsity of the unknown. As practical signals are seldom sparse, sparsity measures other than $\|\cdot\|_{\ell_0}$ e.g., *Gini index* (GI) [25] and *numerical sparsity* [26] have been put forth to compare compressible signals. In this work, we use GI (a normalized measure of sparsity) to compare sparsifying transforms. Consider a vector $\mathcal{I}' = [\mathcal{I}'(0), \mathcal{I}'(1), \dots, \mathcal{I}'(N-1)]$, with its elements re-ordered, such that $|\mathcal{I}'(0)| < |\mathcal{I}'(1)| < \dots < |\mathcal{I}'(N-1)|$. The GI is then defined as

$$\text{GI}(\mathcal{I}') = 1 - 2 \sum_{k=0}^{N-1} \frac{|\mathcal{I}'(k)|}{\|\mathcal{I}'\|_{\ell_1}} \left(\frac{N-k-\frac{1}{2}}{N} \right), \quad (12)$$

where $\|\cdot\|_{\ell_1}$ represents the ℓ_1 norm. One advantage of GI over the conventional norm measures is that it is normalized, and assumes values between 0 and 1 for any vector. Further, it is 0 for the least sparse signal (all coefficients have equal energy) and 1 for the most sparse signal (i.e., all energy concentrated in one coefficient) (see [25] for details). Our numerical findings based on GI suggest that (among the tested transforms) *Haar wavelet* transform [27] maximizes the GI and also satisfies properties i)-iii). As the discussion on all the tested transforms will take us too far afield, we will confine our attention to the sparsifying ability of the Haar transform in comparison with windowing. The unitary Haar transform \mathbf{H}_{haar} can be applied to \mathcal{I}' in a manner identical to (11), i.e.,

$$\mathbf{x}'_{\mathcal{T}} = \Psi_{\mathcal{T}} \mathbf{H}_{haar}^H \mathbf{H}_{haar} \mathcal{I}', \quad (13)$$

where $\mathbf{H}_{haar}^H = \mathbf{H}_{haar}^{-1}$.

4. SIMULATION RESULTS

A 512 sub-carrier SC-FDMA system is simulated, with 2 active users. The channel delay spread is quarter the symbol duration i.e., $N_c = N/4$ and 16-QAM modulation is used. The NBI vector \mathcal{I}_L is obtained from complex normal distribution with SIR=-10dB. Two experiments are conducted that demonstrate the ability of the proposed scheme to successfully recover the NBI in comparison with ℓ_1 -optimization based NBI recovery [9]. In the first experiment no grid offset is assumed, whereas, the second experiment assumes the realistic grid mismatch case.

Reconstruction with No Grid Offset: In this experiment, the number of active NBI sources vary in each symbol with a maximum of four active NBI sources per symbol. The locations of the active NBI sources also vary, however, all NBI sources are restricted to fall on the grid. Fig. 1 presents the BER results vs energy per bit (E_b/N_0) with 64 reserved tones per user (this corresponds to a sub-sampling rate $\frac{|\mathcal{T}'|}{N} = \frac{64}{256} = \frac{1}{4}$). The results depict the ability of the proposed scheme to effectively recover the NBI. Note that there is no visual difference between the reconstruction accuracy of the (*proposed*) scheme and (ℓ_1 -*optimization*). However, the subgraph depicting the average run-time of the (*proposed*) scheme shows that (ℓ_1 -*optimization*) incurs high computational complexity as compared to (*proposed*) by almost two orders of magnitude.

Reconstruction under Grid Offset: In this experiment, first we compare the Haar transform and windowing (Hamming [9]) for their sparsifying ability. The NBI sources are generated with independent grid offset according to (7). The GI is calculated (as a function of active NBI sources) and averaged over 1000 independent runs for \mathcal{I}' and its two transformed counterparts ($\mathbf{H}_{win}\mathcal{I}'$ and $\mathbf{H}_{haar}\mathcal{I}'$). From the results (in Fig. 2), we observe that for a small number of active NBI sources (i.e., ≤ 4) the Haar transform has better sparsifying ability than windowing. Further, the BER performance of proposed SABMP reconstruction scheme for the cases of spread signal (*spread*), windowing (*window*) and Haar transform (*Haar*) is shown in Fig. 3 and is compared with (ℓ_1 -*optimization*) (as a function of E_b/N_0). The ℓ_1 -optimization based NBI recovery is performed using windowing sparsity restoration [9]. A maximum number of four active NBI sources with varying locations and independent frequency offsets per symbol are assumed with sub-sampling rate $1/4$. The lower BER for (*Haar*) transform (in Fig. 3) supports the conclusion that Haar transform possesses better sparsifying characteristics. The low BER is expected as in sparse reconstruction, a scheme better able to sparsify \mathcal{I}' will yield better reconstruction accuracy and hence a lower BER. Further, it is noticed that with grid offset, windowed (ℓ_1 -*optimization*) has an inferior performance to the proposed NBI reconstruction scheme. This behavior is expected, as the performance of ℓ_1 -optimization deteriorates with an increase in the sparsity rate.

5. CONCLUSION

In this paper, we have developed a framework for NBI mitigation in SC-FDMA systems. The proposed approach utilizes the sparsity (or compressibility) of the NBI signal and makes use of a Bayesian algorithm (i.e., SABMP) for the estimation and cancellation of NBI. The SABMP algorithm has several advantages over other sparse reconstruction algorithms, including i) low estimation error, ii) low complexity, and iii) ambivalence to the distribution of the sparse vector. Further, to address the practical issue of grid offset (that destroys the sparsity of the unknown NBI signal), unitary Haar wavelet transform is utilized. Numerical results verify improved performance of Haar transform based sparse NBI recovery using SABMP.

Acknowledgement: The authors would like to acknowledge the support provided by King Fahd University of Petroleum and Minerals (KFUPM) and King Abdulaziz City for Science and Technology (KACST) through the Science and Technology Unit at KFUPM for funding this work.

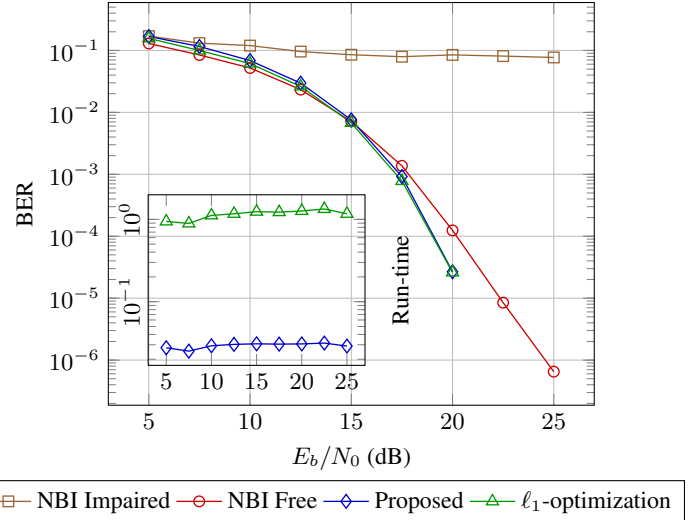


Fig. 1: BER vs E_b/N_0 : $|\mathcal{T}'| = 25\%$, perfect grid alignment.

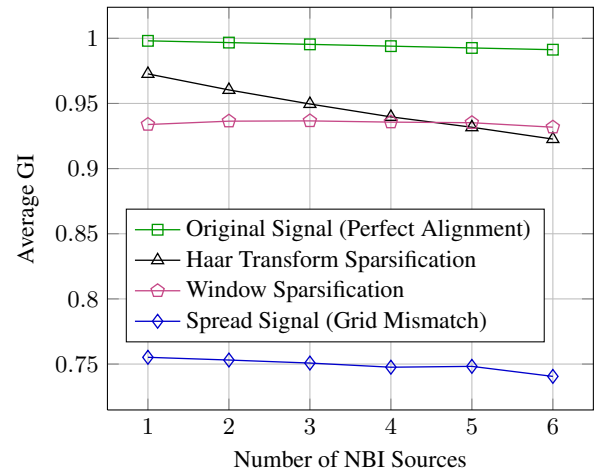


Fig. 2: Average GI vs No. of active NBI sources

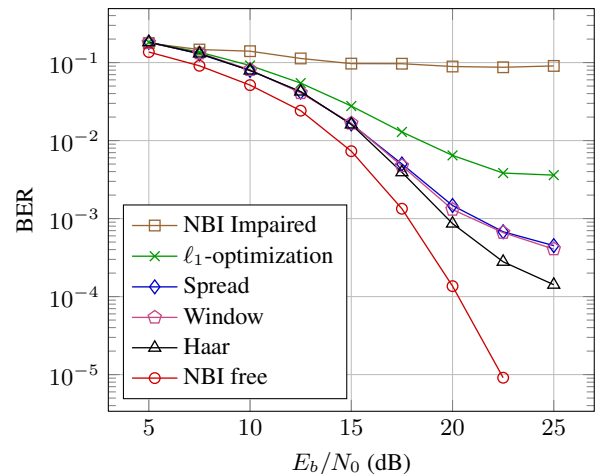


Fig. 3: BER vs E_b/N_0 : $|\mathcal{T}'| = 25\%$, with grid offset.

through project number 09-ELE781-4 as part of the National Science, Technology and Innovation Plan.

6. REFERENCES

- [1] H. G. Myung, J. Lim, and D. Goodman, "Single carrier FDMA for uplink wireless transmission," *IEEE Veh. Technol. Mag.*, vol. 1, no. 3, pp. 30–38, 2006.
- [2] M. Masood and T. Y. Al-Naffouri, "Sparse Reconstruction Using Distribution Agnostic Bayesian Matching Pursuit," *IEEE Trans. Signal Process.*, vol. 61, no. 21, pp. 5298–5309, 2013.
- [3] T. Y. Al-Naffouri, A. A. Quadeer, and G. Caire, "Impulse Noise Estimation and Removal for OFDM Systems," *IEEE Trans. Commun.*, vol. 62, no. 3, pp. 976–989, 2014.
- [4] J. Zhang and J. Meng, "Robust narrowband interference rejection for power-line communication systems using IS-OFDM," *IEEE Trans. Power Del.*, vol. 25, no. 2, pp. 680–692, 2010.
- [5] D. Darsena and F. Verde, "Successive NBI cancellation using soft decisions for OFDM systems," *IEEE Signal Process. Lett.*, vol. 15, pp. 873–876, 2008.
- [6] M. S. Sohail, T. Y. Al-Naffouri, and S. N. Al-Ghadhban, "Narrow Band Interference Cancellation in OFDM: A Structured Maximum Likelihood Approach," in *Proc. IEEE SPAWC*, 2012, pp. 45–49.
- [7] L. Mei, Q. Zhang, X. Sha, and N. Zhang, "WFRFT Precoding for Narrowband Interference Suppression in DFT-Based Block Transmission Systems," *IEEE Commun. Lett.*, vol. 17, no. 10, pp. 1916–1919, 2013.
- [8] M. B. Celebi, I. Guvenc, H. Arslan, and K. A. Qaraqe, "Interference suppression for the LTE uplink," *Phys. Commun.*, vol. 9, pp. 23–44, 2013.
- [9] A. Gomaa and N. Al-Dhahir, "A sparsity-aware approach for NBI estimation in MIMO-OFDM," *IEEE Trans. Wireless Commun.*, vol. 10, no. 6, pp. 1854–1862, 2011.
- [10] A. Ali, M. Masood, M. S. Sohail, S. Al-Ghadhban, and T. Y. Al-Naffouri, "Narrowband Interference Mitigation in SC-FDMA Using Bayesian Sparse Recovery," *arXiv:1412.6137*, 2014.
- [11] G. Berardinelli, B. E. Priyanto, T. B. Sorensen, and P. Mogensen, "Improving SC-FDMA performance by turbo equalization in UTRA LTE uplink," in *Proc. IEEE Veh. Technol. Conf.*, 2008, pp. 2557–2561.
- [12] G. Tang, B. Bhaskar, P. Shah, and B. Recht, "Compressed Sensing Off the Grid," *IEEE Trans. Inf. Theory*, vol. 59, no. 11, pp. 7465–7490, 2013.
- [13] E. J. Candès and M. B. Wakin, "An introduction to compressive sampling," *IEEE Signal Process. Mag.*, vol. 25, no. 2, pp. 21–30, 2008.
- [14] S. Ji, Y. Xue, and L. Carin, "Bayesian compressive sensing," *IEEE Trans. Signal Process.*, vol. 56, no. 6, pp. 2346–2356, 2008.
- [15] J. A. Tropp and A. C. Gilbert, "Signal recovery from random measurements via orthogonal matching pursuit," *IEEE Trans. Inf. Theory*, vol. 53, no. 12, pp. 4655–4666, 2007.
- [16] T. Blumensath and M. E. Davies, "Gradient pursuits," *IEEE Trans. Signal Process.*, vol. 56, no. 6, pp. 2370–2382, 2008.
- [17] D. Needell and J. A. Tropp, "CoSaMP: Iterative signal recovery from incomplete and inaccurate samples," *Appl. Computat. Harmon. Anal.*, vol. 26, no. 3, pp. 301–321, 2009.
- [18] S. D. Babacan, R. Molina, and A. K. Katsaggelos, "Bayesian compressive sensing using Laplace priors," *IEEE Trans. Image Process.*, vol. 19, no. 1, pp. 53–63, 2010.
- [19] N. O'Donoghue and J. M. Moura, "On the product of independent complex Gaussians," *IEEE Trans. Signal Process.*, vol. 60, no. 3, pp. 1050–1063, 2012.
- [20] A. Ali, O. Hammi, and T. Y. Al-Naffouri, "Compressed Sensing Based Joint-Compensation of Power Amplifier's Distortions in OFDMA Cognitive Radio Systems," *IEEE J. Emerg. Sel. Topics Circuits Syst.*, vol. 3, no. 4, pp. 508–520, 2013.
- [21] A. Ali, A. Al-Rabah, M. Masood, and T. Y. Al-Naffouri, "Receiver-based recovery of clipped OFDM signals for PAPR reduction: A Bayesian approach," *IEEE Access*, vol. 2, pp. 1213–1224, 2014.
- [22] H. Zhu, G. Leus, and G. B. Giannakis, "Sparsity-cognizant total least-squares for perturbed compressive sampling," *IEEE Trans. Signal Process.*, vol. 59, no. 5, pp. 2002–2016, 2011.
- [23] H. Zhu, G. B. Giannakis, and G. Leus, "Weighted and structured sparse total least-squares for perturbed compressive sampling," in *Proc. IEEE ICASSP*, 2011, pp. 3792–3795.
- [24] M. Davenport, D. Needell, and M. Wakin, "Signal Space CoSaMP for Sparse Recovery With Redundant Dictionaries," *IEEE Trans. Inf. Theory*, vol. 59, no. 10, pp. 6820–6829, 2013.
- [25] D. Zonoobi, A. A. Kassim, and Y. V. Venkatesh, "Gini index as sparsity measure for signal reconstruction from compressive samples," *IEEE J. Sel. Topics Signal Process.*, vol. 5, no. 5, pp. 927–932, 2011.
- [26] M. Lopes, "Estimating Unknown Sparsity in Compressed Sensing," in *Proc. 30th ICML*, 2013, pp. 1–9.
- [27] A. Haar, "Zur theorie der orthogonalen funktionensysteme," *Mathematische Annalen*, vol. 69, no. 3, pp. 331–371, 1910.